

**ELECTROMAGNETIC DESIGN OF  
HIGH-TEMPERATURE SUPERCONDUCTING  
MICROWAVE FILTERS**

**J.W. Bandler, R.M. Biernacki, S.H. Chen,  
P.A. Grobelny, C. Moskowitz and S.H. Talisa**

**SOS-94-5-R**

**March 1994**

**© J.W. Bandler, R.M. Biernacki, S.H. Chen, P.A. Grobelny, C. Moskowitz and S.H. Talisa 1994**

**No part of this document may be copied, translated, transcribed or entered in any form into any machine without written permission. Address enquiries in this regard to Dr. J.W. Bandler. Excerpts may be quoted for scholarly purposes with full acknowledgement of source. This document may not be lent or circulated without this title page and its original cover.**



**ELECTROMAGNETIC DESIGN  
OF HIGH-TEMPERATURE SUPERCONDUCTING MICROWAVE FILTERS**

J.W. Bandler,\* Fellow, IEEE, R.M. Biernacki,\* Senior Member, IEEE, \*

\* C. Moskowitz\*\*\* and S.H. Talisa,\*\*\*\* Member, IEEE  
S.H. Chen, Member, IEEE W.J. Getsinger, Fellow, IEEE, P.A. Grobelny,

*Abstract*

We present novel approaches to electromagnetic design of high-temperature superconducting quarter-wave parallel coupled-line microstrip filters. The dielectric constant of substrate materials used in high-temperature superconductor technology is too large to be accurately treated by traditional microwave circuit design software packages with analytical/empirical models. We have successfully performed high-temperature superconducting filter design with accurate electromagnetic field simulations. We discuss problems related to electromagnetic design of such filters. We describe a look-up table method and a powerful space mapping optimization technique, which dramatically reduce the CPU time needed in the design process. Finally, we address the issue of improved modeling of the high-temperature superconducting filters using analytical/empirical models.

---

This work was supported in part by the Natural Sciences and Engineering Research Council of Canada under Grants OGP0007239, OGP0042444 and STR0117819; in part by the U.S. Navy under contracts N00014-92-C-2043 and N00014-91-C-0112; and, in part by Optimization Systems Associates Inc.

\* J.W. Bandler, R.M. Biernacki and S.H. Chen are also with Optimization Systems Associates Inc., Dundas, Ontario, Canada L9H 5E7, Tel 905 628 8228.

\*\* W.J. Getsinger, 6662 Bozman-Neavitt Rd., Bozman, MD 21612.

\*\*\* C. Moskowitz is with the Westinghouse Electronic Systems Group, Baltimore, MD 21203.

\*\*\*\* S.H. Talisa is with the Westinghouse Science and Technology Center, Pittsburgh, PA 15235.

## I. INTRODUCTION

The recently discovered high-temperature superconductors (HTS) are of great potential for passive microwave military and commercial applications. Available low-loss and narrow-bandwidth (0.5 - 3%) filter banks are of very large size, which in some satellite and airborne applications is intolerable. Small conventional microstrip filters are too lossy for narrow-band applications. Using HTS technology [1, 2], however, low-loss, narrow-bandwidth microstrip filters, requiring relatively inexpensive cooling, can be made.

Advances in electromagnetic (EM) simulation provide designers the opportunity to accurately simulate passive microstrip circuits. We verified the usefulness of EM simulation in analyzing circuits built with the HTS technology by simulating two existing HTS microstrip filters. In both cases good correlation was observed between the EM simulated and measured responses of the filters.

In this paper we concentrate on the EM design of an HTS quarter-wave parallel coupled-line filter. The difficulty arising here is related to the large dielectric constant of the substrate materials ( $\epsilon_r \approx 24$ ) used in the HTS technology and the inability of the traditional microwave circuit design techniques to analyze structures built of such materials. This is especially true for narrow-band, parallel coupled-line filters where loose coupling between sections is required. To overcome this problem we resort to EM field simulations. EM simulations can provide results that are in good agreement with experimental data. This, however, is at the expense of very high computational cost. This limitation shows up very clearly in analysis of narrow-bandwidth filters whose inherent high sensitivity calls for a very fine grid in the numerical EM simulation.

In order to decrease the CPU time required and overcome the high sensitivity of the filter we considered two approaches. The first approach is based on a table of coupling versus gap and frequency values and the second is based on a novel space mapping (SM) circuit optimization [3]. In the look-up table approach we analyze the couplings in different sections of the filter for different gaps in each of the sections swept over the frequency band of interest. The couplings are

determined from EM simulations and the table is iteratively updated. In the SM approach an adaptive mapping between an OSA90/hope [4] simulation model and *em* [5, 6] simulation is established. Such a mapping, adaptively refined during optimization, allows us to benefit from the accuracy of EM simulation while using a much faster model for optimization. The SM method is a novel extension of our work on optimization-driven EM simulation [7, 8]. The method was tested using OSA90/hope interfaced to *em* through Empipe [9].

In Section II we describe the filter to be designed. In Section III we show the inability of the traditional simulators with analytical/empirical models to accurately model the HTS filter. Section IV includes examples verifying the usefulness of EM simulators in analyzing HTS filters. In this section we also discuss some issues specific to EM simulation of the HTS filters. In Section V we describe problems associated with utilizing geometrical interpolation in conjunction with EM simulations to design the HTS filter. The new look-up table method and SM optimization technique as applied to the design of the HTS filter are described in Sections VI and VII, respectively. Section VIII contains a discussion on improving the analytical/empirical model of the filter. Finally, Section IX contains our conclusions.

## II. THE FILTER

We wish to design a four-pole quarter-wave parallel coupled-line microstrip filter. The geometry of the filter is shown in Fig. 1.  $L_1$ ,  $L_2$  and  $L_3$  are the lengths of the parallel coupled-line sections and  $S_1$ ,  $S_2$  and  $S_3$  are the gaps between the sections. The width  $W$  is the same for all the sections as well as for the input and output microstrip lines  $L_0$ . The thickness of the lanthanum aluminate substrate used is 20 mil and the dielectric constant is assumed to be 23.425. The design specifications are as follows.

$$|S_{21}| \leq 0.05 \quad \text{for} \quad f \leq 3.967 \text{ GHz and } f \geq 4.099 \text{ GHz}$$

$$|S_{21}| \geq 0.95 \quad \text{for} \quad 4.008 \text{ GHz} \leq f \leq 4.058 \text{ GHz}$$

This corresponds to a 1.25% bandwidth.  $L_1, L_2, L_3, S_1, S_2$  and  $S_3$  are the design parameters.  $L_0$  and  $W$  are fixed.

We approach design of the filter by employing both the traditional analytical/empirical models and EM simulations.

### III. FILTER DESIGN USING TRADITIONAL SIMULATORS

Computer aided filter design involves minimization of a scalar objective function  $U$  which is a measure of the deviation of the filter responses from the imposed design specifications. In order to formulate  $U$  we consider error functions defined as

$$e_j(\mathbf{x}) = R_j(\mathbf{x}) - S_{uj} \quad \text{or} \quad e_j(\mathbf{x}) = S_{lj} - R_j(\mathbf{x}) \quad (1)$$

where  $S_{uj}$  and  $S_{lj}$  are the upper and lower specifications, respectively, and  $R_j(\mathbf{x})$  is the response of the filter at a given point of designable variables  $\mathbf{x}$ . Errors  $e_j(\mathbf{x})$  are computed at frequencies for which  $S_{uj}$  and/or  $S_{lj}$  are specified. A negative error value indicates that the corresponding specification is satisfied. For positive error values the corresponding specifications are violated.

The objective function  $U$  may be the generalized  $\ell_p$  function [10] defined as

$$U = \begin{cases} \left[ \sum_{j \in J} e_j(\mathbf{x})^p \right]^{1/p} & \text{if } \mathbf{x} \notin A \\ - \left[ \sum_{j=1}^M -e_j(\mathbf{x})^{-p} \right]^{-1/p} & \text{if } \mathbf{x} \in A \end{cases} \quad (2)$$

where the index set  $J$  is given as

$$J = \{ j \mid e_j(\mathbf{x}) \geq 0 \} \quad (3)$$

and the acceptability region  $A$  is defined as

$$A = \{ \mathbf{x} \mid e_j(\mathbf{x}) < 0 \quad j = 1, 2, \dots, M \} \quad (4)$$

$M$  is the total number of error functions. By letting  $p = \infty$  we have the minimax objective

$$U = \max_j e_j(\mathbf{x}) \quad (5)$$

which is used in our design of the HTS filter.

We started the design of our HTS filter by optimizing the filter using two commercial microwave CAD packages, namely, OSA90/hope and Touchstone [11]. The minimax solutions are listed in the first two columns of Table I. Subsequently, we performed *em* simulations at both solutions. The *em* simulation results differed from the circuit simulation results and did not satisfy the specifications. The  $|S_{21}|$  and  $|S_{11}|$  responses are shown in Figs. 2 and 3. EM verification confirms that traditional simulators may fail to provide accurate solutions in the design of HTS filters. However, they can be used as a tool to obtain a starting point for further EM based design.

#### IV. EM SIMULATION OF HTS FILTERS

To investigate the usefulness of EM simulation in analyzing circuits built in the HTS technology we simulated and measured two existing HTS microstrip filters. The filters together with the corresponding measurements and EM simulation results are shown in Figs. 4 and 5. In both cases good correlation can be observed between the measured and simulated responses. The shapes of the responses are nearly identical. The frequency shift between the measured and simulated responses is most likely due to the discrete nature of the numerical EM analysis introducing rounding of the geometrical dimensions of the filters to the EM simulation grid (see Section V) and/or to using a simulation grid which was not fine enough.

The simulation grid, or simply grid, is defined by the user and is imposed on the analyzed structure during numerical EM analysis. Subsequent computations are performed at the grid points.

In general, using a finer grid (larger number of grid points) makes the analysis time longer and the analysis results more accurate. Using a coarser grid (smaller number of grid points) shortens the analysis time but may degenerate the accuracy of the results. Therefore, it is very important to select a grid that would make EM analysis not only as efficient as possible but also sufficiently accurate.

While investigating different grid sizes for the analysis of the HTS quarter-wave parallel coupled-line microstrip filter we observed that the accuracy of the results depended heavily on the grid size used in the EM analysis. Since the grid used by the *em* [5] simulator is uniform we need two grid spacings  $\Delta x$  and  $\Delta y$  to define the grid.

Fig. 6 shows the EM simulated responses of  $|S_{21}|$  of the filter in an early stage of the design process obtained using different grids. In particular, we fixed the grid spacing in the  $x$  direction at  $\Delta x = 5$  mil and used three different grid spacings in the  $y$  direction:  $\Delta y_1 = 3.5$  mil,  $\Delta y_2 = 1.75$  mil and  $\Delta y_3 = 0.875$  mil. For all three grids the geometry of the circuit was kept unchanged with the following values of the geometrical parameters:  $L_0 = 50$  mil,  $W = 7$  mil,  $L_1 = L_2 = L_3 = 190$  mil,  $S_1 = 21$  mil,  $S_2 = 94.5$  mil and  $S_3 = 108.5$  mil. It can be seen from Fig. 6 that using different grid sizes preserved the shape of the response but resulted in a shifts of the center frequency of the filter. Moreover, comparing the responses obtained using grid spacings  $\Delta y_1$  and  $\Delta y_2$  and then  $\Delta y_2$  and  $\Delta y_3$  shows that the difference in the shift becomes smaller for smaller grid spacings.

This phenomenon forces the user to use a finer grid for EM simulations in order to preserve the accuracy of the results. This becomes even more significant when EM simulators are applied to HTS filters. Very small bandwidths make the circuits very sensitive. For other applications a 10 MHz shift in the center frequency, as observed in Fig. 6, could be negligibly small but for the HTS filter under consideration it corresponds to 20% of the bandwidth.

In our analysis we set the grid spacings to  $\Delta x = 1$  mil and  $\Delta y = 1.75$  mil. This resulted in approximately one CPU hour needed to simulate the filter at a single frequency on a Sun SPARCstation 10.

## V. ELECTROMAGNETIC DESIGN WITH GEOMETRICAL INTERPOLATION

One of the main problems in utilizing EM simulators in the design of HTS filters is the discrete nature of the numerical EM analysis. Numerical EM analysis can only be performed for discrete or on-the-grid values of the parameters defining the geometry of the circuit. Whenever a response for an off-the-grid point is required we employ geometrical interpolation to estimate the response. Utilizing geometrical interpolation makes it possible to provide a gradient based optimizer with continuous responses and smooth gradients of the responses [7, 8].

Geometrical interpolation applied to typical microwave circuits proved to be efficient and accurate [7, 8]. However, it failed when applied to the HTS filter design. Fig. 7 explains why. It shows three  $|S_{21}|$  responses of the filter obtained for three different points, i.e., sets of the geometrical parameters. The grid spacings used are  $\Delta x = 2.5$  mil and  $\Delta y = 1.75$  mil. Two of the points are on-the-grid points and the third one is an off-the-grid point. Geometrical interpolation is used to approximate the response at the off-the-grid point. Parameters  $L_0, W, S_1, S_2, S_3$  are set to 50, 7, 21, 94.5 and 108.5 mil, respectively and they have the same values at all three points. For the first on-the-grid point  $L_1 = L_2 = L_3 = 190$  mil and for the second on-the-grid point  $L_1 = L_2 = L_3 = 192.5$  mil. For the off-the-grid point  $L_1 = L_2 = L_3 = 191.25$  mil. As shown in Fig. 7, the responses for the on-the-grid points are typical filter responses with similar passband widths but shifted center frequencies. The significant shift of the center frequency not only proves high sensitivity of the circuit but also makes geometrical interpolation inaccurate. The interpolated response for the off-the-grid point has a much wider passband with a deep notch in the passband. The accuracy of the interpolation could be improved by using much finer grid spacings but this would make the EM simulation time prohibitively long.

With this experience we set out to develop new methods for adapting the traditional analytical/empirical models and the electromagnetic field simulators for the design of HTS filters.

## VI. FILTER DESIGN USING THE LOOK-UP TABLE METHOD

Although the technique is general in nature, it has been applied only to the class of filters known as parallel coupled-line filters which are derivable from lowpass ladder networks. One starts with the normalized lowpass ladder network elements which satisfy some predetermined shape requirement and results in the lowpass prototype element values also known as the  $g$  values. An appropriate bandpass and impedance transformation is performed which leads to good approximations of the even and odd mode impedances of the coupled-line sections which comprise the filter. The next step in the design process is to determine the geometry or conductor arrangement which realizes this set of even/odd mode impedances. The medium that we have chosen is microstrip on 20 mil lanthanum aluminate. In this medium, the coupled sections are characterized by three geometric parameters; line width, coupling length and coupling gap, which must be chosen to provide the required even and odd mode impedances. The ratio of these impedances depends only on the coupling coefficient of the coupler and the product depends on the impedance level.

The simulator aided design process consists of estimating the quarter wavelength in the medium at filter band center, and the gap required for the coupling. One then constructs a model for the field simulator which consists of a coupled-line with input and output ports on a diagonal with the other diagonal remaining as open circuits. Actually, several models are constructed over a range of gaps so that one can interpolate the *em* simulator's results to the required gap based upon the required coupling factor. This process is repeated for each coupled section of the filter. When a complete set of gaps has been determined by interpolation, the filter is modeled for analysis by the field simulator. The result usually has a shape that is close to the desired shape but is offset in center frequency. The amount of the frequency error and the original coupling length provide enough information to compute a length correction, i.e., the fractional change in frequency is proportional to the negative of the fractional change in length.

The process is then repeated using the new coupling length. We have found adequate convergence after three iterations.

The filter's  $|S_{21}|$  and  $|S_{11}|$  responses simulated by *em* at the look-up table method solution are shown in Figs. 8 and 9, respectively. The solution point is listed in the third column of Table I. The  $|S_{21}|$  response has the desired shape but the center frequency is slightly shifted w.r.t. specifications. Also, a small ripple present in the passband, see Fig. 8(b), results in non-uniform  $|S_{11}|$  in the passband.

## VII. FILTER DESIGN USING THE SPACE MAPPING METHOD

In the SM optimization technique [3] we create and iteratively refine a mapping

$$\mathbf{x}_{OS} = T(\mathbf{x}_{EM}) \quad (6)$$

from the EM simulator input space  $\{\mathbf{x}_{EM}\}$  to the optimization system (OS) parameter space  $\{\mathbf{x}_{OS}\}$ . The SM technique does not impose any restrictions on the type of the mapping. In order to find the mapping an overdetermined system of equations may have to be solved. In such situations, optimization techniques, such as least-squares, can be used. Though not necessary, it is desirable that  $T$  is invertible. If so, the inverse mapping  $T^{-1}$  is used to find the image of the optimal OS solution  $\mathbf{x}_{OS}^*$ , namely,

$$\bar{\mathbf{x}}_{EM} = T^{-1}(\mathbf{x}_{OS}^*) \quad (7)$$

$T$  is established through an iterative process. The initial mapping  $T^{(0)}$  is found using a preselected set  $\mathbf{B}_{EM}$  of  $k$  points in the EM input space and the set  $\mathbf{B}_{OS}$  of corresponding points in the OS parameter space. The points in  $\mathbf{B}_{OS}$  are determined such that

$$f_{OS}(\mathbf{x}_{OS}^i) \approx f_{EM}(\mathbf{x}_{EM}^i), \quad i = 1, 2, \dots, k \quad (8)$$

where  $f_{OS}$  and  $f_{EM}$  are the circuit responses simulated by the OS and EM simulators, respectively. At the  $j$ th iteration  $B_{EM}$  is expanded by the new image of  $\mathbf{x}_{OS}^*$  computed using  $(T^{(j)})^{-1}$  and  $B_{OS}$  is expanded accordingly. The iterations continue until

$$f_{EM}(\bar{\mathbf{x}}_{EM}) \approx f_{OS}(\mathbf{x}_{OS}^*) \quad (9)$$

Applying the SM optimization technique to the design of the HTS filter we used the Empipe [9] interface interconnecting *em* to OSA90/hope. All the processing needed to establish the mapping was performed within the OSA90/hope environment.

A total of 13 *em* simulations was sufficient to establish the mapping  $T$  which satisfies (9). To satisfy the match implied by (8) we used the  $\ell_1$  optimizer. For a matching problem the  $\ell_1$  objective is defined by

$$U = \sum_{j=1}^M |e_j| \quad (10)$$

where  $M$  is the number of error functions, which are derived directly from (8). The properties of the  $\ell_1$  objective are superior in data fitting, parameter extraction and other applications involving matching of responses. The point  $\bar{\mathbf{x}}_{EM}$  obtained as the  $(T)^{-1}$  image of  $\mathbf{x}_{OS}^*$  is listed in the fourth column of Table I. It gave us an excellent response of the filter, as simulated by *em*. The  $|S_{21}|$  response, shown in Fig. 10, meets the design specifications well. The  $|S_{11}|$  response, shown in Fig. 11, is also improved.

### VIII. IMPROVING THE ANALYTICAL/EMPIRICAL MODEL OF THE FILTER

It is desirable to create a fast and accurate model of the HTS filter for the optimal set of the parameter values. Such a model can be used for efficient analysis of the filter especially in situations where the filter is a subcircuit of a larger circuit.

Fig. 12 compares the optimal  $|S_{21}|$  response of the filter obtained using OSA90/hope [4] analytical/empirical microstrip models with the EM simulated SM solution. Good agreement can

be observed in the passband region but the responses become significantly different for the stopband frequencies. In particular, there is a notch in the EM simulated response which is completely missing in the analytical/empirical model response. Similar notch or notches are observed in measurements of other microstrip filters (see Figs. 1 and 2). The presence of the notch(es) in the filter response is undesirable.

The generation of notch(es) is related to the ground currents from the coaxial line into the box with the filter which divide unevenly, most going below the substrate, but some going to the box lid and sides. The currents can be taken as analogous to small dipoles over the distances they flow. The sum of the currents can be taken as analogous to a single dipole over the full height of the box, driven at the level of the unbalanced current exciting the longitudinal section magnetic (LSM) mode. Thus, there are two signal paths from one connector to the other: the microstrip mode goes via the filter and the LSM mode goes via the box. When the two signals are equal and opposite in sign they cancel, causing a notch in the stopband.

We expanded the analytical/empirical model by adding a lumped inductor directly between the input and the output of the filter. Subsequently, we optimized the value of the inductance of the additional inductor so that the responses of the analytical/empirical model of the filter best match the EM simulated responses of the filter. We used the  $\ell_1$  optimizer for optimization. The optimal value of the inductor is  $L = 0.43 \mu\text{H}$ . The match between the responses of the analytical/empirical model with the inductor and the EM model is very good. It is shown in Fig. 13. To model the phenomena related to the ground currents by a single lumped inductor is a simplified approach. Nonetheless, the resulting model of the filter is quite accurate.

## IX. CONCLUSIONS

We have demonstrated the difficulties of the traditional analytical/empirical models to accurately model narrow-band quarter-wave parallel coupled-line microstrip filters built using the HTS technology. We have addressed problems associated with utilizing EM simulations in design

of such filters. In particular, we have discussed the influence of the size of the EM simulation grid and the discrete nature of the numerical EM analysis. We have shown how geometrical interpolation, introduced to overcome the discretization problem, may fail due to the high sensitivity of HTS filters. Subsequently, we have presented two new EM-based methods for CAD of narrow-band parallel coupled-line microstrip filters built using the HTS technology. The new space mapping optimization method is a general approach which can be applied to other design problems. It is especially attractive for designs involving CPU intensive simulators, where it substantially decreases the number of necessary simulations. Finally, we have presented an improved analytical/empirical model of the filter. Further study on the analytical/empirical as well as EM modeling of the HTS narrow-band parallel coupled-line microstrip filters will aim at elimination of the undesirable notch(es) in the response of the filter.

#### REFERENCES

- [1] S.H. Talisa, M.A. Janocko, C. Moskowitz, J. Talvacchio, J.F. Billing, R. Brown, D.C. Buck, C.K. Jones, B.R. McAvoy, G.R. Wagner and D.H. Watt, "Low- and high-temperature superconducting microwave filters," *IEEE Trans. Microwave Theory Tech.*, vol. 39, 1991, pp. 1448-1454.
- [2] W.G. Lyons, R.R. Bonetti, A.E. Williams, P.M. Mankiewich, M.L. O'Malley, J.M. Hamm, A.C. Anderson, R.S. Withers, A. Meulenberg and R.E. Howard, "High- $T_c$  superconductive microwave filters," *IEEE Trans. Magnetics*, vol. 27, 1991, pp. 2537-2539.
- [3] J.W. Bandler, R.M. Biernacki, S.H. Chen, P.A. Grobelny and R.H. Hemmers, "Space mapping technique for electromagnetic optimization," submitted to this issue of *IEEE Trans. Microwave Theory Tech.*, 1994.
- [4] *OSA90/hope™*, Optimization Systems Associates Inc., P.O. Box 8083, Dundas, Ontario, Canada L9H 5E7, 1993.
- [5] *Em User's Manual and Xgeom User's Manual*, Sonnet Software, Inc., 135 Old Cove Road, Suite 203, Liverpool, NY 13090-3774, 1992.
- [6] J.C. Rautio and R.F. Harrington, "An electromagnetic time-harmonic analysis of arbitrary microstrip circuits," *IEEE Trans. Microwave Theory Tech.*, vol. 35, 1987, pp. 726-730.
- [7] J.W. Bandler, S. Ye, R.M. Biernacki, S.H. Chen and D.G. Swanson, Jr., "Minimax microstrip filter design using direct EM field simulation," in *IEEE MTT-S Int. Microwave Symp. Dig.* (Atlanta, GA), 1993, pp. 889-892.

- [8] J.W. Bandler, R.M. Biernacki, S.H. Chen, P.A. Grobelny and S. Ye, "Yield-driven electromagnetic optimization via multilevel multidimensional models," *IEEE Trans. Microwave Theory Tech.*, vol. 41, 1993, pp. 2269-2278.
- [9] *Empipe™*, Optimization Systems Associates Inc., P.O. Box 8083, Dundas, Ontario, Canada L9H 5E7, 1993.
- [10] J.W. Bandler and S.H. Chen, "Circuit optimization: the state of the art," *IEEE Trans. Microwave Theory Tech.*, vol. 36, 1988, pp. 424-443.
- [11] *Touchstone® Reference Manual Version 3.0*, EEsof, Inc., 5601 Lindero Canyon Road, Westlake Village, CA 91362-4020, 1991.

TABLE I  
HTS PARALLEL COUPLED-LINE MICROSTRIP  
FILTER DESIGN RESULTS

Parameter (mil)	OSA90/hope Optimization	Touchstone Optimization	Look-up Table Method	SM Method
$L_1$	191.00	188.70	188.70	190.00
$S_1$	21.74	22.52	20.88	19.25
$L_2$	195.58	188.11	188.10	192.00
$S_2$	96.00	93.19	76.02	75.25
$L_3$	191.00	188.58	188.59	189.00
$S_3$	114.68	109.13	85.07	91.00
$W$	7.00	6.93	6.93	7.00
$L_0$	50.00	50.00	50.00	50.00

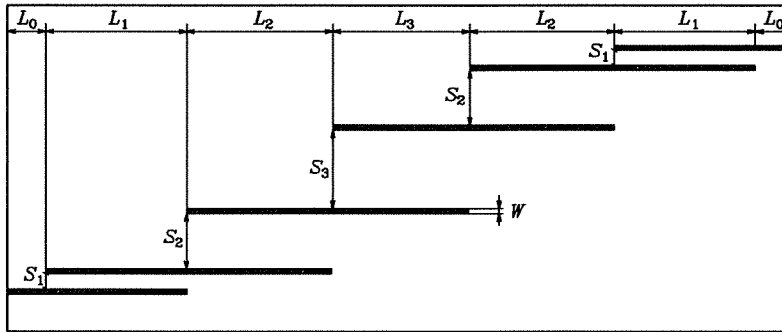
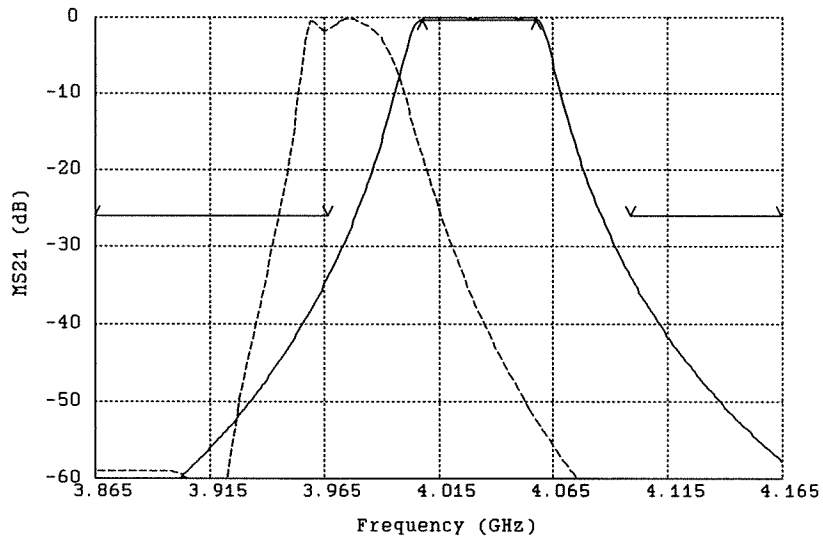
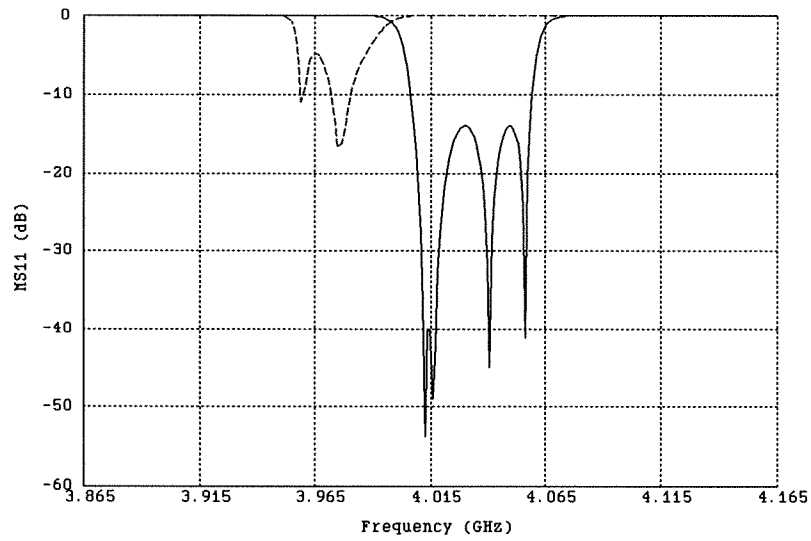


Fig. 1. The structure of the HTS quarter-wave parallel coupled-line microstrip filter (to scale). The dielectric constant and the substrate thickness are 23.425 and 20 mil, respectively. The geometrical dimensions are listed in Table I. The  $x$  and  $y$  grid sizes for *em* simulations are 1.0 and 1.75 mil. About 1 CPU hour is needed for analysis at a single frequency on Sun SPARCstation 10.

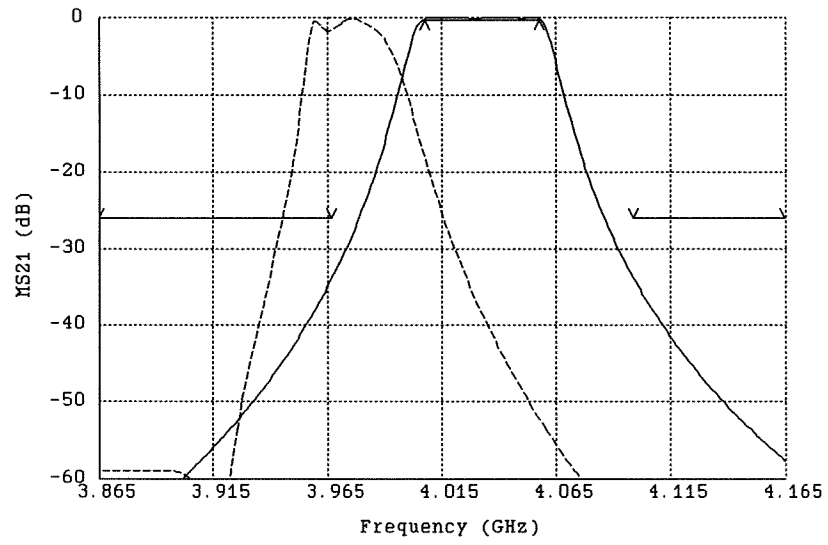


(a)

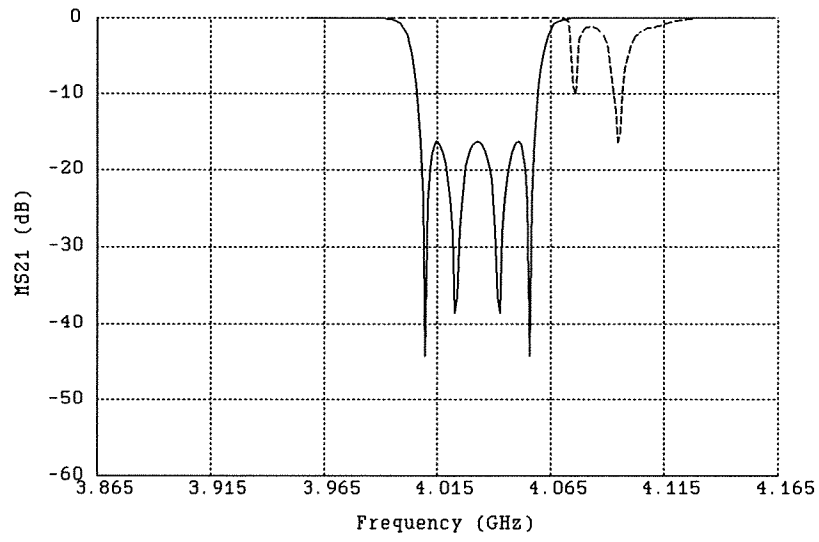


(b)

Fig. 2. The optimal solutions (solid lines) of (a)  $|S_{21}|$  and (b)  $|S_{11}|$  obtained using OSA90/hope. The corresponding *em* simulation results are shown as dashed lines.  $\nabla$  indicate upper and  $\wedge$  indicate lower specifications.



(a)

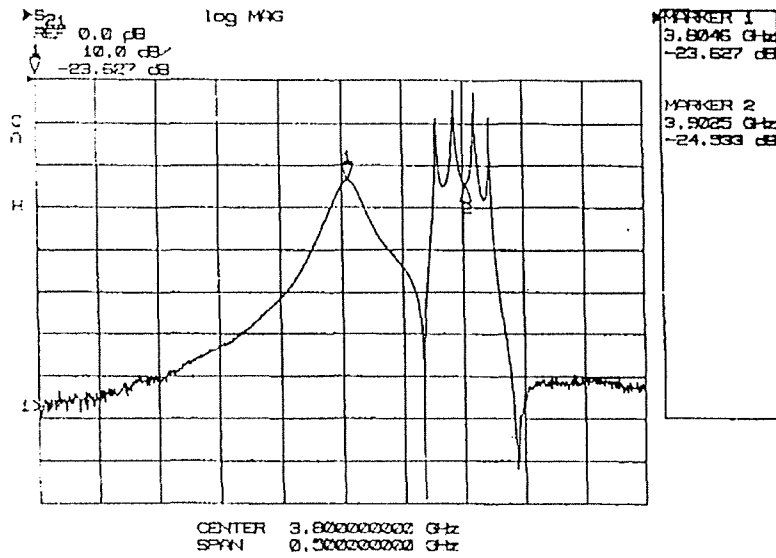


(b)

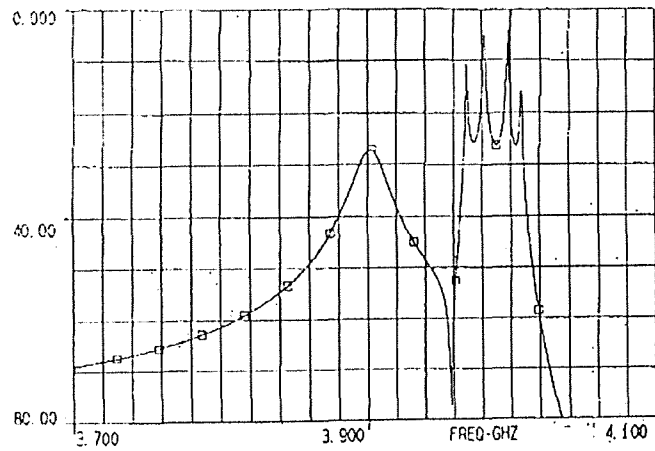
Fig. 3. The optimal solutions (solid lines) of (a)  $|S_{21}|$  and (b)  $|S_{11}|$  obtained using Touchstone. The corresponding *em* simulation results are shown as dashed lines.  $\nabla$  indicate upper and  $\wedge$  indicate lower specifications.



(a)

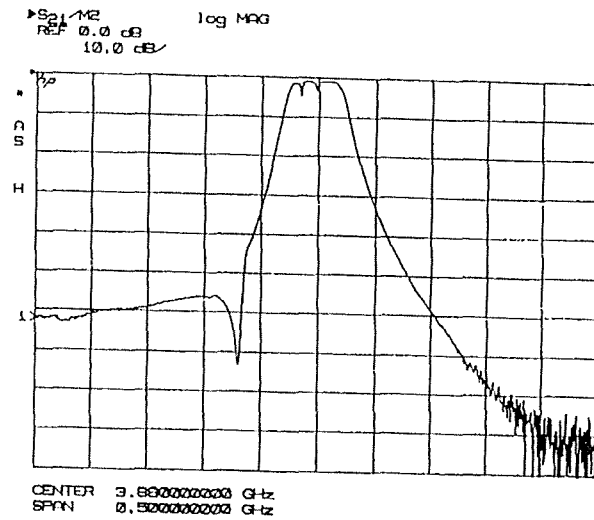
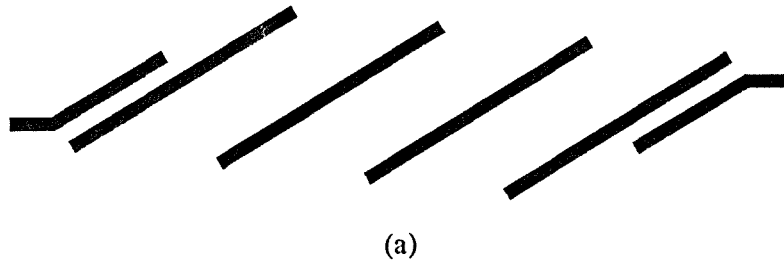


(b)

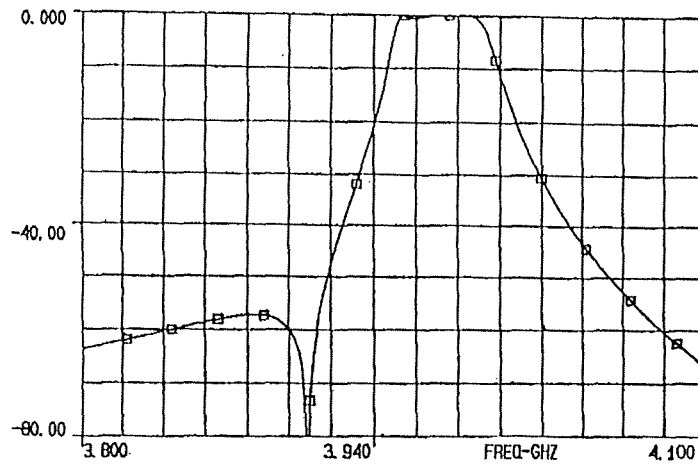


(c)

Fig. 4. Comparison between measured and EM simulated responses of the HTS filter shown in (a). (b) and (c) show measured and *em* simulated responses, respectively.



(b)



(c)

Fig. 5. Comparison between measured and EM simulated responses of the HTS filter shown in (a). (b) and (c) show measured and *em* simulated responses, respectively.

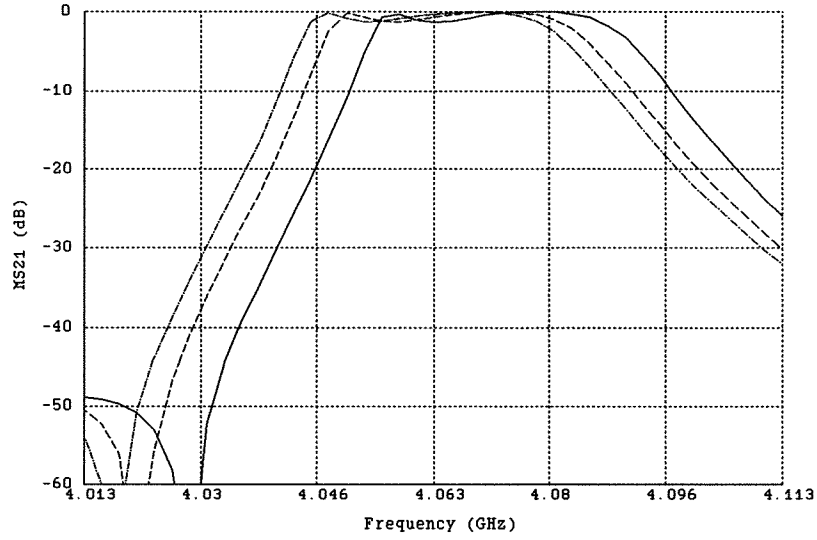


Fig. 6. The *em* simulated  $|S_{21}|$  response of the HTS parallel coupled-line filter obtained in an early stage of the design process for different grid sizes. The grid size in the  $x$  direction is  $\Delta x = 5$  mil and it is kept fixed. The grid sizes in the  $y$  direction are  $\Delta y_1 = 3.5$  mil (solid line),  $\Delta y_2 = 1.75$  mil (dashed line) and  $\Delta y_3 = 0.875$  mil (dotted line).

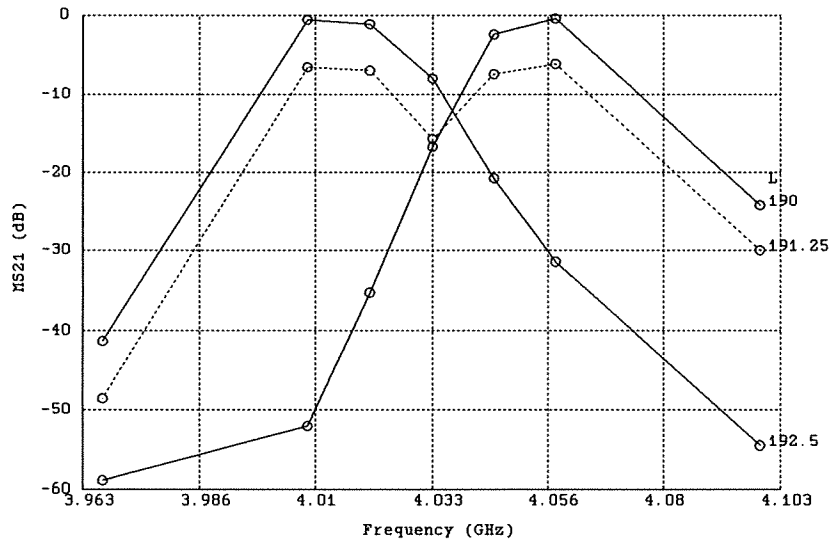
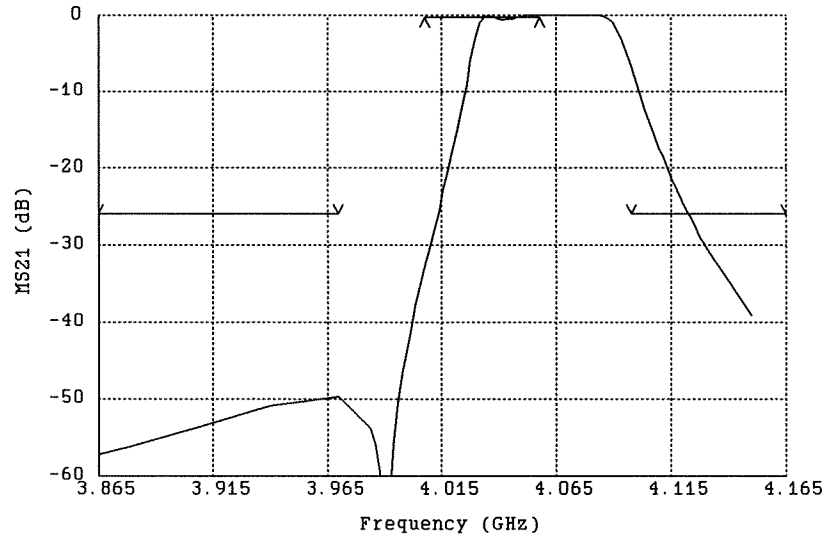
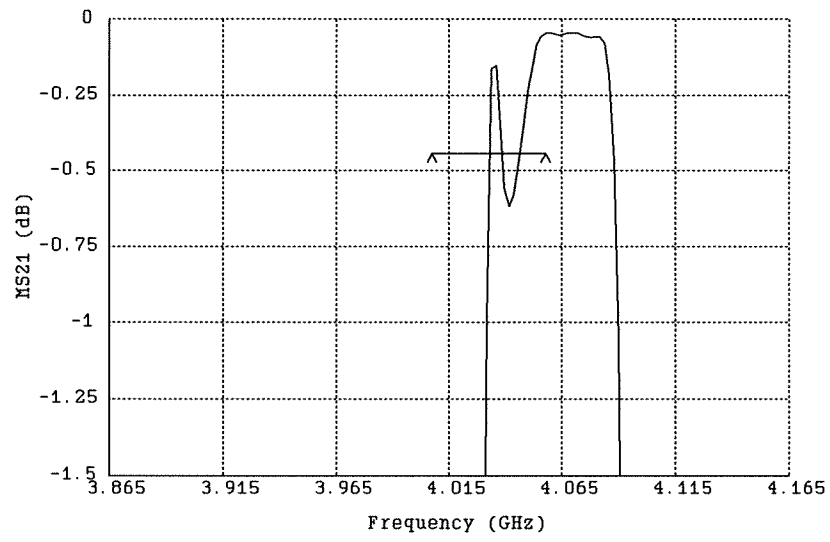


Fig. 7. Illustration of utilizing the geometrical interpolation in the design of the HTS parallel coupled-line microstrip filter. The  $|S_{21}|$  responses for  $L_1 = L_2 = L_3 = L = 190$  and  $192.5$  mil (solid lines) do not involve geometrical interpolation. The response for  $L_1 = L_2 = L_3 = L = 191.25$  mil (dashed line) is interpolated and clearly incorrect. Circles indicate analyzed frequency points.



(a)



(b)

Fig. 8. The *em* simulated  $|S_{21}|$  response of the HTS parallel coupled-line filter at the solution obtained using the look-up table method. (a) Response for the overall band. (b) Passband details of the response.  $\nabla$  and  $\wedge$  indicate upper and lower specifications, respectively. The response exhibits the desired shape with slightly shifted center frequency.

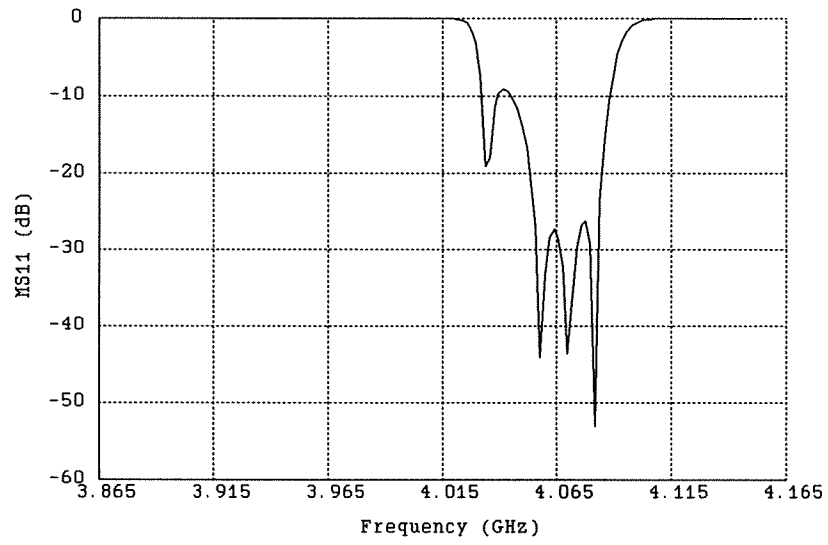
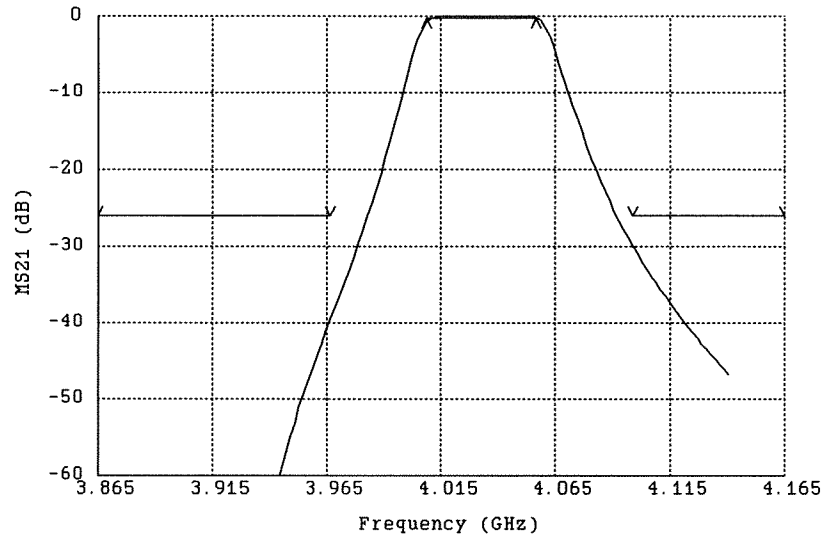
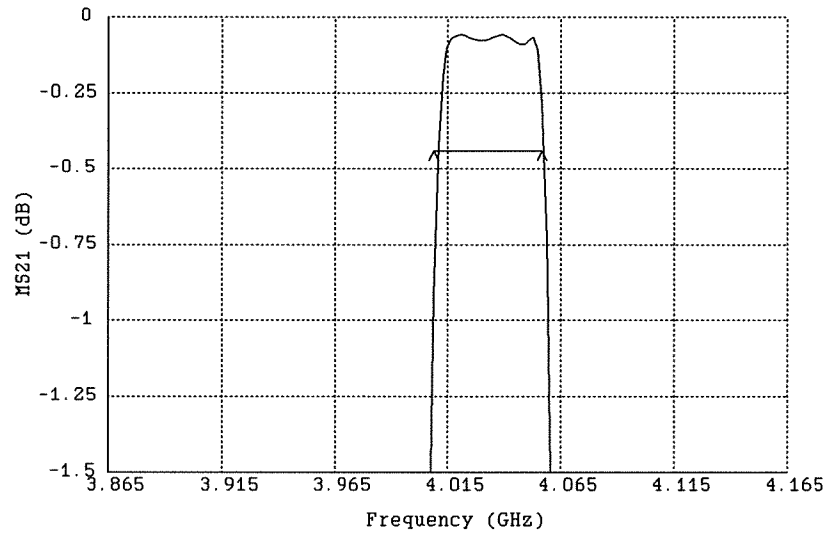


Fig. 9. The *em* simulated  $|S_{11}|$  response of the HTS parallel coupled-line filter at the solution obtained using the look-up table method.



(a)



(b)

Fig. 10. The *em* simulated  $|S_{21}|$  response of the HTS parallel coupled-line filter at the solution obtained using the SM optimization method. (a) Response for the overall band. (b) Passband details of the response.  $\nabla$  and  $\wedge$  indicate upper and lower specifications, respectively.

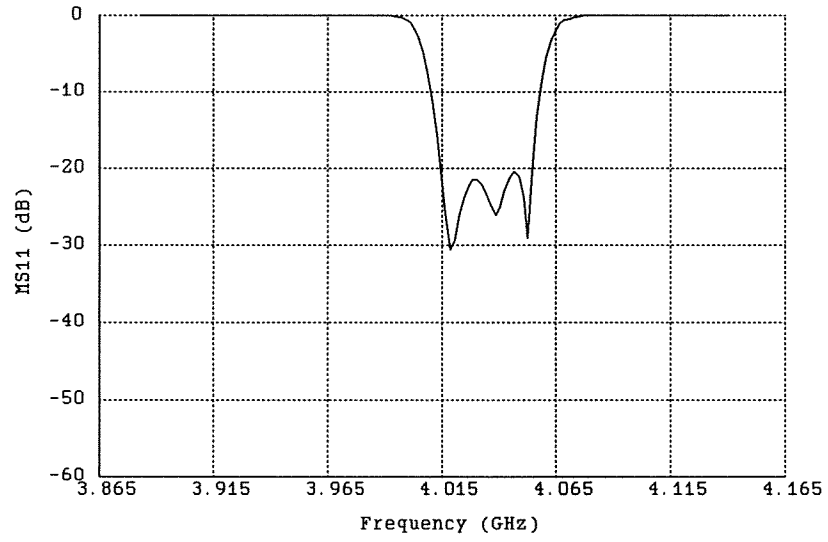
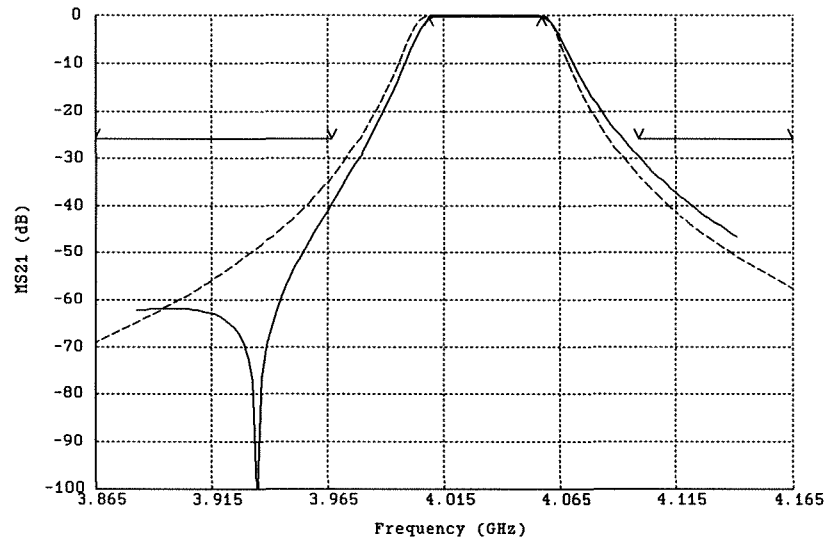
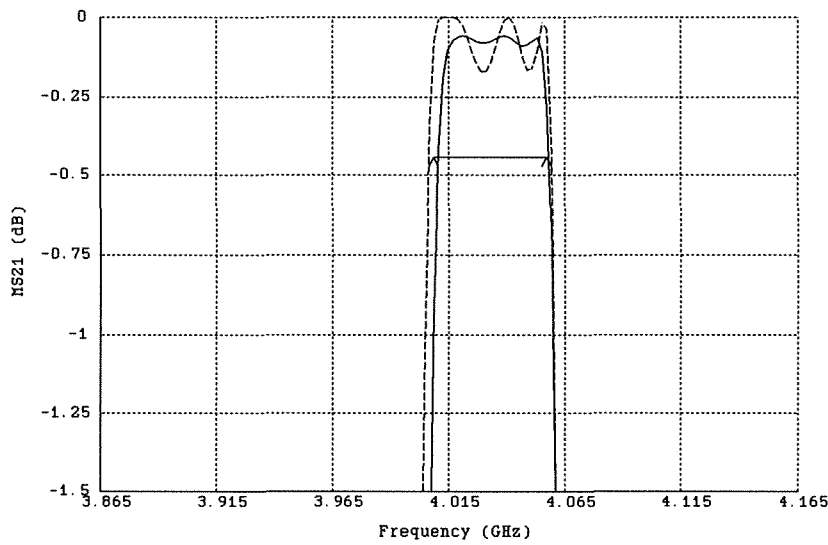


Fig. 11. The *em* simulated  $|S_{11}|$  response of the HTS parallel coupled-line filter at the solution obtained using the SM optimization method.

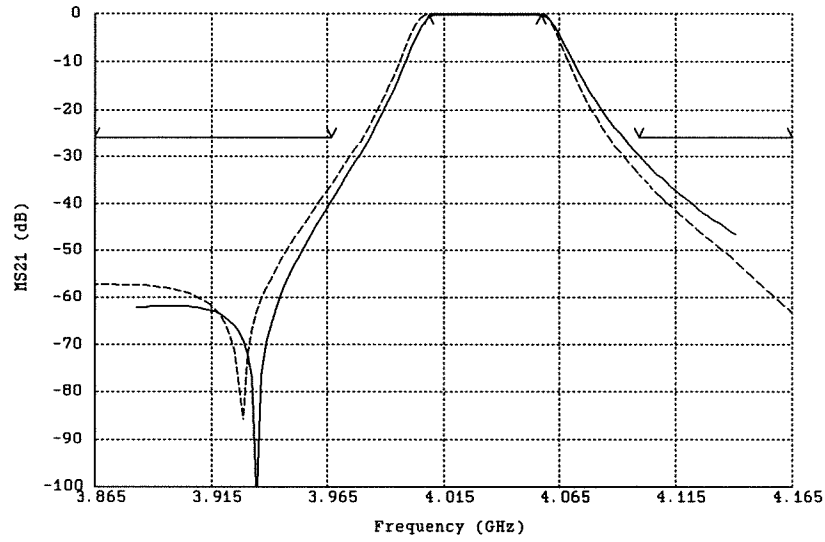


(a)

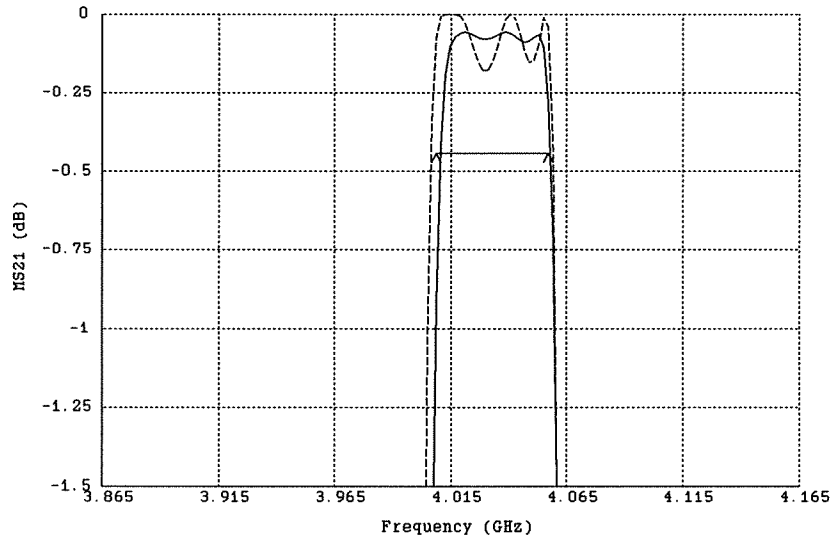


(b)

Fig. 12. Comparison between the optimal  $|S_{21}|$  response of the HTS parallel coupled-line filter obtained using the analytical/empirical model (dashed line) and the EM simulated SM solution (solid line). (a) Response for the overall band. (b) Passband details of the response.



(a)



(b)

Fig. 13. Modeling of the notch in the  $|S_{21}|$  response of the HTS parallel coupled-line filter. In order to model the notch we introduced an additional inductor between the input and output of the filter. The analytical/empirical model response is shown as a dashed line. The EM simulated response is shown as a solid line. (a) Response of the overall band. (b) Passband details of the response.